Organic & Biomolecular Chemistry

Accepted Manuscript

This article can be cited before page numbers have been issued, to do this please use: A. V. Kletskov, A. D. Zatykina , M. V. Grudova, A. A. Sinelshchikova, M. Grigoriev , V. P. Zaytsev, D. M. Gil, R. A. Novikov, F. I. Zubkov and A. Frontera, *Org. Biomol. Chem.*, 2020, DOI: 10.1039/D0OB01201G.

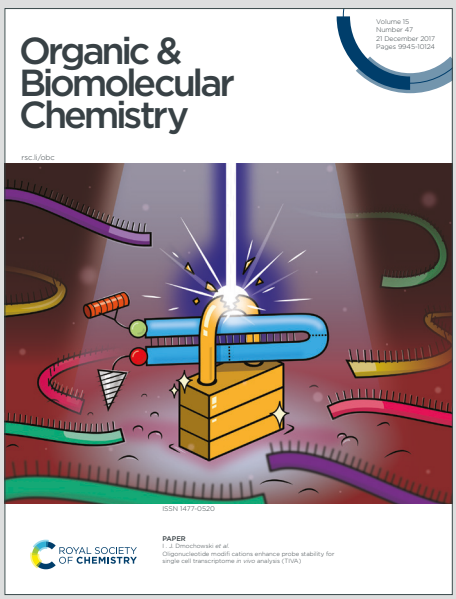

ROYAL SOCIETY OF CHEMISTRY

rsc.li/obc

View Article Online
DOI: 10.1039/D0OB01201G

ARTICLE

Raise the anchor! Synthesis, X-ray and NMR characterization of 1,3,5-triazinanes with an axial *tert*-butyl group

Received 00th January 20xx,
Accepted 00th January 20xx

DOI: 10.1039/x0xx00000x

Alexey V. Kletskov,[a] Anastasya D. Zatykina,[a] Mariya V. Grudova,[a] Anna A. Sinelshchikova,[b] Mikhail S. Grigoriev,[b] Vladimir P. Zaytsev,[a] Diego M. Gil,[c] Roman A. Novikov,[d] Fedor I. Zubkov,[a,*] and Antonio Frontera[e,*]

***N*-*t*-Bu-*N'*,*N''*-disulfonamide-1,3,5-triazinanes were synthesized and characterized by X-ray single crystal structure analysis. In the course of the X-ray structure elucidation, the first solid experimental evidence of the axial position of the *tert*-butyl group in unconstrained hexahydro-1,3,5-triazacyclohexanes was obtained. Dynamic low-temperature NMR analysis allowed to fully investigate a rare case of crystallization-driven unanchoring of the *tert*-butyl group in the chair conformation of saturated six-membered cycles. DFT calculations show that the use of explicit solvent molecules is necessary to explain the equatorial position of the *t*-Bu group in solution. Otherwise, the axial conformer is the thermodynamically stable isomer.**

Introduction

It is a well-known fact that the *tert*-butyl group, being one of the most sterically bulky substituents due to the high energy of the 1,3-diaxial repulsion (4.9 kcal/mol), is a conformational anchor in the chair conformation of cyclohexanes and many other saturated six-membered cycles.[1] Obviously, this adverse interaction can be significantly reduced in six-membered rings bearing no axial hydrogen atoms in 3 and 5 positions, relative to the *t*-Bu substituent. 1,3,5-Triazinanes are typical representatives of such ring systems; due to the low inversion barrier, they can exist in the form of conformers with both axially and equatorially oriented substituents at nitrogen atoms. However, even for these conformationally mobile molecules, rigorous evidence of the axial location of the *tert*-butyl group could not have been obtained before. In this regard, the main goal that we pursued in this work was the study of the conformation equilibrium of 1,3,5-triazinane rings bearing an N-*tert*-butyl group in the solid phase and in solutions.

The theoretical dispute on the possibility of the axial location of the *tert*-butyl group in the chair conformation of saturated six-membered heterocycles was started in the middle of the 20th century by one of the founders of modern dynamic stereochemistry, Ernest Eliel.[2] And to date there are quite a few publications in which the axial orientation of substituents could be detected in a solution with the help of the dipole moment measurement,[3] NMR spectroscopy[4,5] or molecular mechanics calculations (Scheme 1).[4,6]

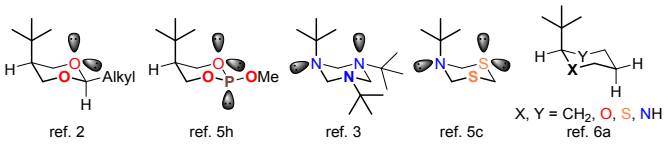

ref. 2 ref. 5h ref. 3 ref. 5c ref. 6a

Scheme 1. Selected six-membered perhydro heterocycles for which the axial arrangement of the *tert*-butyl group was theoretically predicted.

According to the data obtained in these works, usually in a solution of such cycles an equilibrium between axial and equatorial conformers exists due to the rapid chair-to-chair inversion of the cycle. Similar cases were previously predicted[5b,f,7] for 1,3,5-triazacyclohexanes bearing bulky *N*-alkyl substituents and the *tris*(4-bromophenyl) substituted analog.[8]

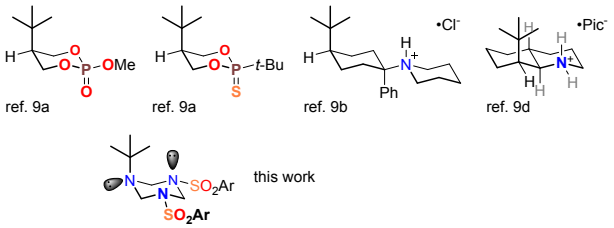

ref. 9a ref. 9a ref. 9b ref. 9d

Scheme 2. Six-membered saturated cycles with the axial arrangement of the *tert*-butyl group proved by the X-ray analysis.

[a] *Organic Chemistry Department, Faculty of Science, Peoples' Friendship University of Russia (RUDN University), 6 Miklukho-Maklaya St., Moscow 117198, Russian Federation. E-mail: fzubkov@sci.pfu.edu.ru*
[b] *Frumkin Institute of Physical Chemistry and Electrochemistry, Russian Academy of Sciences, Leninsky pr. 31, bld. 4, Moscow 119071, Russian Federation.*
[c] *INBIOFAL (CONICET - UNT), Instituto de Química Orgánica - Cátedra de Química Orgánica I, Facultad de Bioquímica, Química y Farmacia, Universidad Nacional de Tucumán, Ayacucho 471 (T4000INI), San Miguel de Tucumán - Tucumán – Argentina*
[d] *N.D. Zelinsky Institute of Organic Chemistry, Russian Academy of Sciences, 47 Leninsky Pr., Moscow 119991, Russian Federation*
[e] *Department of Chemistry, Universitat de les Illes Balears, Crta. de Valldemossa km 7.7, 07122 Palma de Mallorca (Baleares), Spain. E-mail: toni.frontera@uib.es*
Electronic Supplementary Information (ESI) available: [details of any supplementary information available should be included here]. See DOI: 10.1039/x0xx00000x

It should be said as well that, to the moment, very limited X-ray data on the saturated six-membered rings bearing the *tert*-butyl group in the axial position were reported (Scheme 2).[9] They are: *trans*-5-*tert*-butyl-2-methoxy-2-oxo- and *cis*-2,5-di-*tert*-butyl-2-thio-1,3,2-dioxaphosphorinanes,[9a] *cis*-1-(4-(*tert*-butyl)-1-phenylcyclohexyl)piperidine hydrochloride[9b], 5-*tert*-butyl-tetrahydro-1,3,5-triazine-2(1*H*)one[9c] (flattened cycle with a pseudo axial *t*-Bu group) and (4a*RS*,8*RS*,8a*RS*)-8-(*tert*-butyl)decahydroquinolin-1-ium picrate[9d] (constrained cycle). Herein we report the first solid evidence for an axial position of the *tert*-butyl group in unconstrained 1,3,5-triazinanes.

Results and Discussion

As it was elucidated in the recent review,[11f] 1,3,5-triazinanes have found extensive applications as two-, three-, four-, and six-atom synthons for the construction of various nitrogen-containing heterocycles. Hereat, as the analysis of the data of the above-mentioned review shows, symmetrically substituted hexahydro-1,3,5-triazines are the most often used objects of these transformations, which is associated with their greater availability. Chemical transformations of asymmetrically substituted triazinanes have been much less studied due to the absence of general preparative methods for their preparation. Besides, the latter might possess biological activity different from that of symmetrical hexahydro-1,3,5-triazines, thus representing not so well studied objects for bioscreening.

During our attempts to transform 3-*tert*-butyl-1,5,3-dioxazepane (**6**) into the corresponding 1,5,3-dioxazepanes[10] we found out that in the case of using sulfamides **5** as an amine component, triazinanes (**1–4**) are formed (Scheme 3).[11]

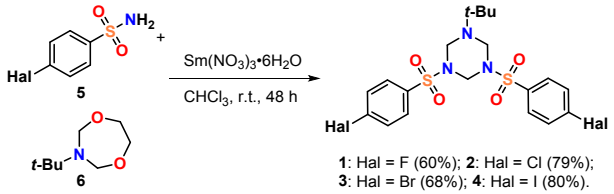

Scheme 3. Synthesis of 1,3,5-triazinanes (**1**–**4**) on the basis of 3-(*tert*-butyl)-1,5,3-dioxazepane (**6**) and sulfonamides (**5**).

The proposed mechanism of the 1,5,3-dioxazepane transformation is presented in Scheme 4 (see the ESI for the discussion).

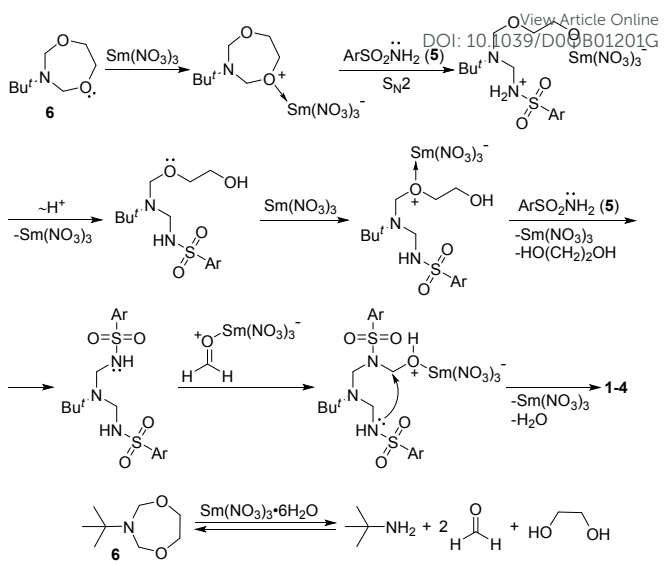

Scheme 4. Plausible mechanism of 1,3,5-triazinanes (**1–4**) formation.

X-Ray analysis of synthesized triazinanes (**1–4**) revealed three essential details. Firstly, the molecules **1** and **2** can crystallize with or without the presence of the co-crystallized solvent molecule of $CDCl_3$ that does not much change the geometry of F and Cl substituted triazinanes **1·CDCl₃** and **2·CDCl₃** in the crystal state (Fig. 1). Secondly, in all the cases in the solid phase the *tert*-butyl group is in the axial position of the triazinane ring, *i.e*. each molecule of **1–4**, **1·CDCl₃** and **2·CDCl₃** prefers the 1*a*,3*e*,5*e*-chair conformation **C** where two halogenophenylsulfonyl substituents are in the equatorial position, while the *tert*-butyl group is located axially (Scheme 5).

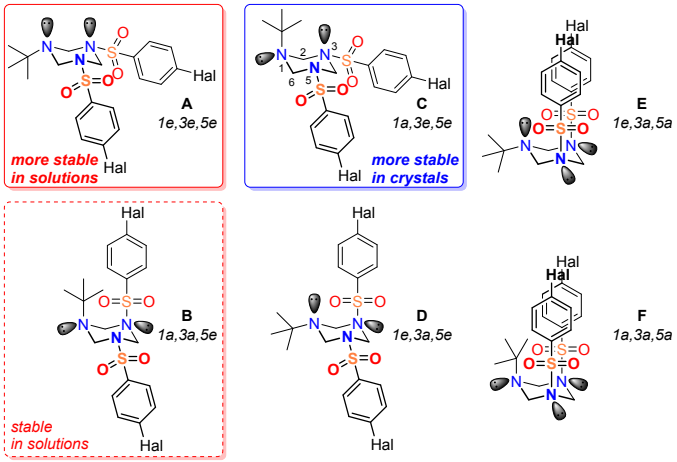

Scheme 5. Possible chair conformers of triazinanes **1**–**4**. Conformer **C** with the 1*a*,3*e*,5*e*-arrangement of substituents are realized in the solid state, conformers **A** (1*e*,3*e*,5*e*) and **B** (1*a*,3*a*,5*e*) predominate in solutions at the temperatures below –100 °C.

It should be emphasized that the observed conformation **C** is one of the six possible conformations **A–F** theoretically possible for the chair conformation of 1,3,5-triazacyclohexanes **1–4** (Scheme 5).

View Article Online
DOI: 10.1039/D0OB01284C

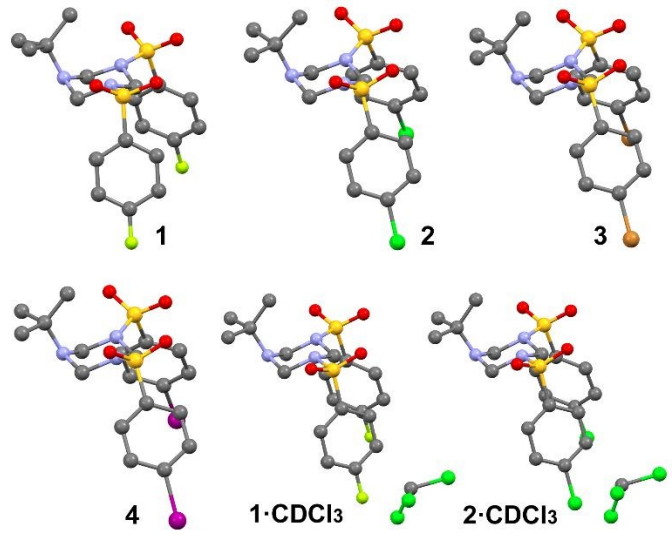

Fig. 1 X-ray structure of compounds **1–4**, **1·CDCl$_3$** and **2·CDCl$_3$** reported herein. The hydrogen atoms were deleted for clarity.

Thirdly, it is known that depending on substituents, the nitrogen atom in sulfonamides can exist in both sp^2 and sp^3 hybridizations.[12] The analysis of the values of valence angle sums at the sulfonamide N-3 and N-5 atoms allows to conclude that they have a pyramidal configuration and, therefore, the sp^3 hybridization (the sum of the valence angles fluctuates roughly between 345–350° for all molecules). The N-1 atom connected to the *t*-Bu group has the same pyramidal configuration with the same geometrical parameters. Thus, we can assume that the triazinane cycles of all molecules **1–4**, **1·CDCl$_3$** and **2·CDCl$_3$** have the classical, practically undistorted chair conformation **C** in the crystalline state (Fig. 1 and Scheme 5).

The X-ray data obtained here for the first time provided reliable evidence of the axial position of the *tert*-butyl group in the 1,3,5-triazacyclohexane ring. It is likely that the axial orientation of the *tert*-butyl group in the solid phase observed in this case could be explained by the higher ability of axial conformers to crystalize compared to the equatorial ones.

It will be interesting to compare the data of this study with our precedent work published,[11e] where triazinanes similar to compounds **1**–**4** were synthesized and another unusual phenomenon, a sp^2-sp^3 disequalization of chemically identical sulfonamide nitrogen atoms was examined.

Crystallographic analysis

The packing of triazacyclohexanes without a co-crystallized solvent molecule (structures **1–4**) is governed by non-classical C–H···O hydrogen bonds, which, along with the presence of substituted heteroatoms in the cycle, contributes to the slight deviation of geometrical parameters from a similar conformation of cyclohexane. Compounds **2–4** form 1D chains along the [001] direction due to hydrogen bonds between CH_2 groups of triazinane cycle and O atoms of adjacent molecules (Fig. 2a). At the same time, another motif of C–H···O hydrogen bonding implements along the [100] direction due to the contacts between CH of phenyl rings and oxygen atoms (Fig. 2b). Considering all the hydrogen bonds, the molecules form the plane layers in (010) (Figs. 3 and S1, S2). All distances for hydrogen bonds are presented in Table S2.

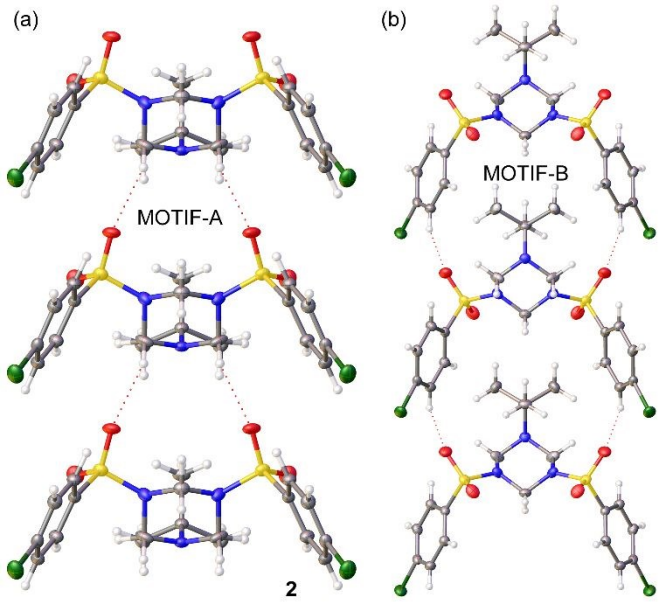

Fig. 2 X-ray packing due to C–H···O hydrogen bonds of **2** (the same packing is present in **3** and **4**), (a) 1D chains along [001] direction, view along *a*, (b) 1D chains along [100] direction, view along *c*.

Compound **1** forms 1D chains in the [001] direction due to the hydrogen bonds between CH_2 groups and O atoms of adjacent molecules (similar for compounds **2–4**). However, the molecules in the chain alternate the orientation and are twisted differently from **2–4** (Fig. S3).

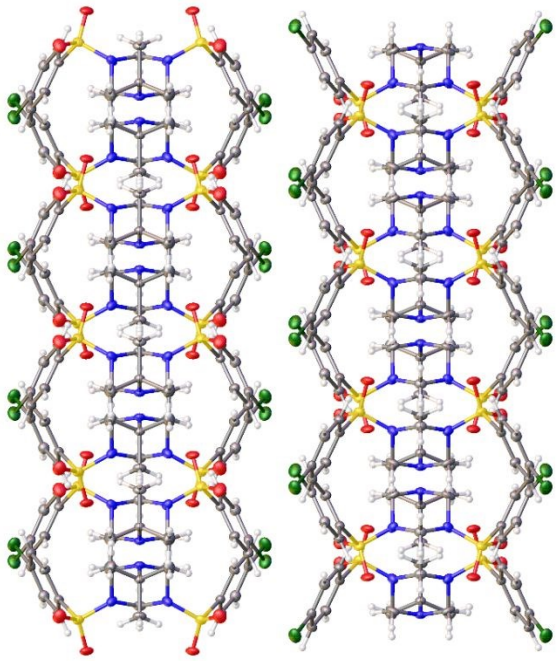

Fig. 3 X-ray packing of **2** (the same packing is present in **3** and **4**) showing side view of two layers, view along *a*.

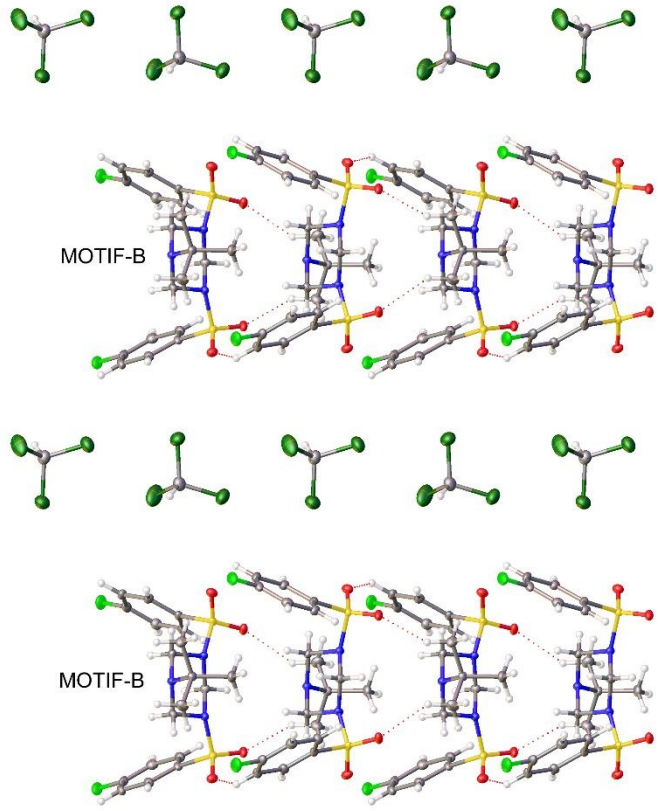

Fig. 4 X-ray packing of **1·CDCl$_3$** showing the alternation of **MOTIF-B** chains and $CDCl_3$ chains, view along *b*.

The packing of solvates **1·CDCl$_3$** and **2·CDCl$_3$** is different from unsolvated molecules **1**, **2** (and **3**, **4** as well) because Cl-containing guest-molecules of the solvent begin to interact strongly with host molecules. The main crystallographic feature of the solvates is the presence of 1D chains created by chloroform molecules due to Cl···Cl halogen bonds (Table S3). Triazinane molecules pack forming 1D channels for chloroform chains (Fig. 4), and chloroform chains interact with triazinane columns by HBs binding them together (Table S3).

Although compounds **1·CDCl$_3$** and **2·CDCl$_3$** are isostructural, one can find different intermolecular contacts in the structures. In the crystal packing of triazinane **1·CDCl$_3$** molecules form 1D chains along the [100] direction due to C–H···O hydrogen bonds between CH-groups of phenyl rings and oxygen atoms (Fig. S4, Tables S2, S3). The molecules in the chain are connected by the screw axis 2_1, therefore the orientation of neighboring molecules is alternating (Fig. 4) and the distance between them is half of the translation *a*. These chains are parallel to chloroform chains. The chains are held together due to the C–H···F hydrogen bonds where the fluorine atom plays the role of acceptor (Table S3).

In structure **2·CDCl$_3$** it is also possible to find triazinane columns along the [100] direction where alternating molecules are connected by screw axis 2_1, however, HBs between CH-groups of phenyl rings and oxygen atoms are longer than in **1·CDCl$_3$** (Fig. S5a, Table S3). In contrast to **1·CDCl$_3$** there are specific intermolecular C–Cl···O interactions in the crystal of **2·CDCl$_3$** (Table S3), which stabilize 2D layers in the (100) plane (Fig. S5b). Additional C–H···Cl hydrogen bonds where the chlorine atom plays the role of acceptor stabilize the structure (Table S3).

NMR studies

The previously mentioned XRD analysis of triazinanes **1**–**4** allowed us to detail their spatial structure in the solid phase, in particular, to establish the axial position of the *tert*-butyl group in the six-membered ring unequivocally, but, as it is well known, the conformation of molecules in the solid state is often dramatically different from that in solutions.[1d,e] In order to complete the picture, at the next logical continuation of the work we carried out a conformational analysis of the objects of this investigation in solutions with the aid of dynamic NMR spectroscopy.[13] All synthesized triazinanes **1**–**4** were analyzed using the full set of 2D NMR methods and demonstrated very similar behavior in solutions of deuterated dichloromethane in a wide range of temperatures. Hereby, the spectral data obtained for sulfamide **1** turned out to be the most informative due to the presence of fluorine atoms in its molecule. Thus, only the NMR data of compound **1** will be discussed below for brevity of the following reasoning.

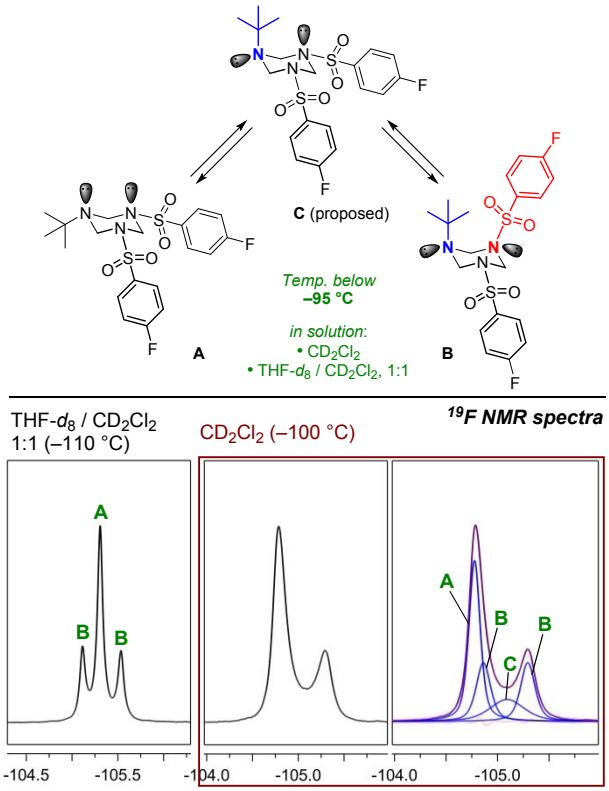

Fig. 5 *At the top*. Equilibrium between conformers **A**–**C** of triazinane **1** in solution at the temperatures below –95 °C, detected by advanced NMR analysis. *At the bottom*. Key ^{19}F NMR spectra of the conformers **A**–**C**: in THF-d_8 / CD_2Cl_2 (at –110 °C left), and in CD_2Cl_2 (at –100 °C middle and right). Right ^{19}F spectrum is presented in the form of deconvolution signals (components are indicated in blue) and assignments. Conformers ratio **A/B/C**: in THF-d_8/CD_2Cl_2 (v/v, 1:1) = **59/41/<5**; in CD_2Cl_2 = **43/40/17**. Structure of conformer **C** is proposed.

DOI: 10.1039/D0OB01201G

Only one set of narrow and well-resolved signals from all hydrogen, fluorine and carbon nuclei is observed in the spectra of *bis*-*N*-fluorobenzenesulfonyl substituted 1,3,5-triazinane **1** at 20–25 °C in both $CDCl_3$ and CD_2Cl_2 (see the ESI). As it will be discussed below, this situation is a reflection of the rapid transition between all possible conformers of the molecule at r.t and this is the cause of the averaging of chemical shifts of all atoms belonging to the different conformers. Hence, we have studied in detail the conformations of compound **1** in a solution using dynamic low temperature NMR spectroscopy on ^{1}H, ^{13}C, and ^{19}F nuclei (Figs. 5 and 6).

The first experiments showed that the energetic barrier between the possible conformations of the molecule is too small, which leads to the need for using very low temperatures. CD_2Cl_2, one of the most available and convenient deuterated solvents with the lowest melting point, turned out to be insufficient because it freezes in an NMR tube at *ca.* –100 °C. Specially used for such purposes *i*-PrCl-d_7 (m.p is *ca.* –130 °C) and $CDFCl_2$ prepared using a literature method[14] (m.p is *ca.* –135 °C) dissolve triazinane **1** (as well as the most part of other compounds) very poorly at room and especially at low temperatures, and therefore they are not applicable for NMR experiments in high resolution. Moreover, $CDFCl_2$, which is quite often used in the literature for dynamic NMR experiments,[13,14] is a gas at room temperature, which greatly complicates the work with it. So, in this study we have found and used for the first time the eutectic solvent mixture of THF-d_8/CD_2Cl_2 (v/v, 1:1), which has the glass transition temperature in an NMR tube below –125 °C and allows to record NMR spectra down to almost –140 °C (Fig. 6). It should be emphasized, that it is sufficient for solving most problems of dynamic NMR, and besides, –140 °C is the low temperature limit for most modern commercial conventional NMR probes. We suppose that the found solvent system is more convenient from a practical point of view, since it allows to avoid the use of non-deuterated freons gaseous under normal conditions, such as $CHClF_2$ (m.p −175 °C, b.p −41 °C) and CCl_2F_2 (m.p −156 °C, b.p −30 °C), which were employed in sealed NMR tubes for the same purposes previously.[4] Similarly, the toluene-d_8/CD_2Cl_2 system (m.p is *ca.* –120 °C)[15] is also hardly applicable in this case due to the low solubility of tested triazinanes **1–4**.

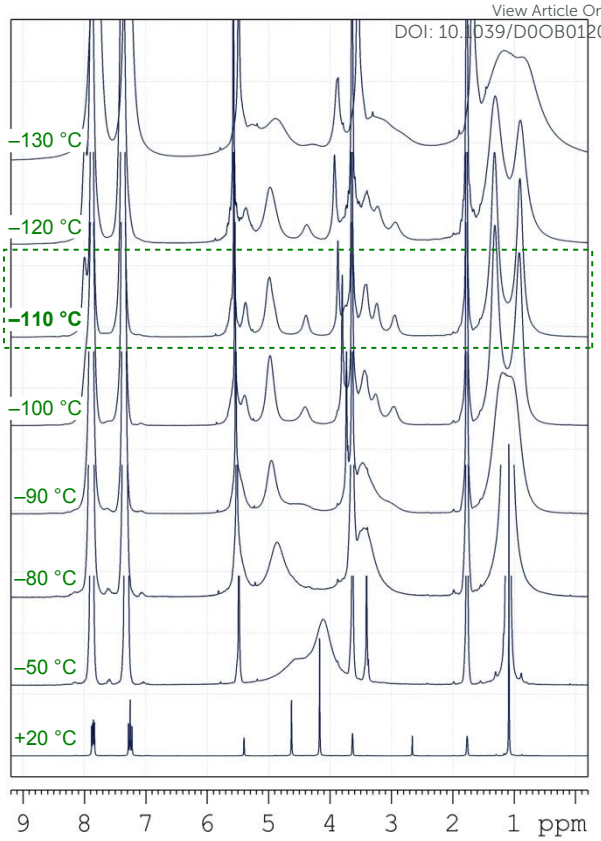

Figure 6. A set of ^{1}H NMR spectra of the fluorotriazine **1** in THF-d_8/CD_2Cl_2 (1:1) at various temperatures (from +20 °C to –130 °C). It can be seen that the best separation of two conformers **A** and **B** is achieved at –110 °C, after which the conformational equilibrium becomes more complicated with the manifestation of more subtle effects. As a result, the signals are noticeably broadened again below –120 °C, including the effect of an increase in solvent viscosity near the freezing point.

Taking into account that ^{19}F nuclei are the best for the observation of the temperature dynamic, we have studied the conformational equilibrium of triazinane **1** on these nuclei in two solvents: in CD_2Cl_2 to –100 °C, and in the mixture of THF-d_8/CD_2Cl_2 (v/v, 1:1) to –135 °C (Fig. 5 and 6). In both solvents, the coalescence point and separation of conformer signals begin below *ca.* –95 °C (see ESI), however, conformer compositions were different in each solvent (Fig. 5). Besides the predominant all-*e* conformer **A**, we have detected two additional conformers **B** and **C**. Both minor conformers **B** and **C** have axial *t*-Bu groups, while conformer **B** also possesses the additional axial *p*-$FC_6H_4SO_2$ group (Fig. 5). As a result, two different *p*-$FC_6H_4SO_2$ substituents and two ^{19}F signals are observed in the spectra of conformer **B**. In the mixture of THF-d_8/CD_2Cl_2 (v/v, 1:1) an almost clear picture of the signals of two conformers **A** and **B** was detected (Fig. 5, from the bottom left). In CD_2Cl_2 the corresponding ^{19}F spectrum consists of four signals with a strong overlap of the peaks belonging to all three conformers **A–C** (Fig. 5, from the bottom right). The deconvolution processing[16] allows to undoubtedly extract all signals and to accurately analyze the spectrum in combination with 2D NMR techniques and changes at various temperatures.

View Article Online
DOI: 10.1039/D0OB01301G

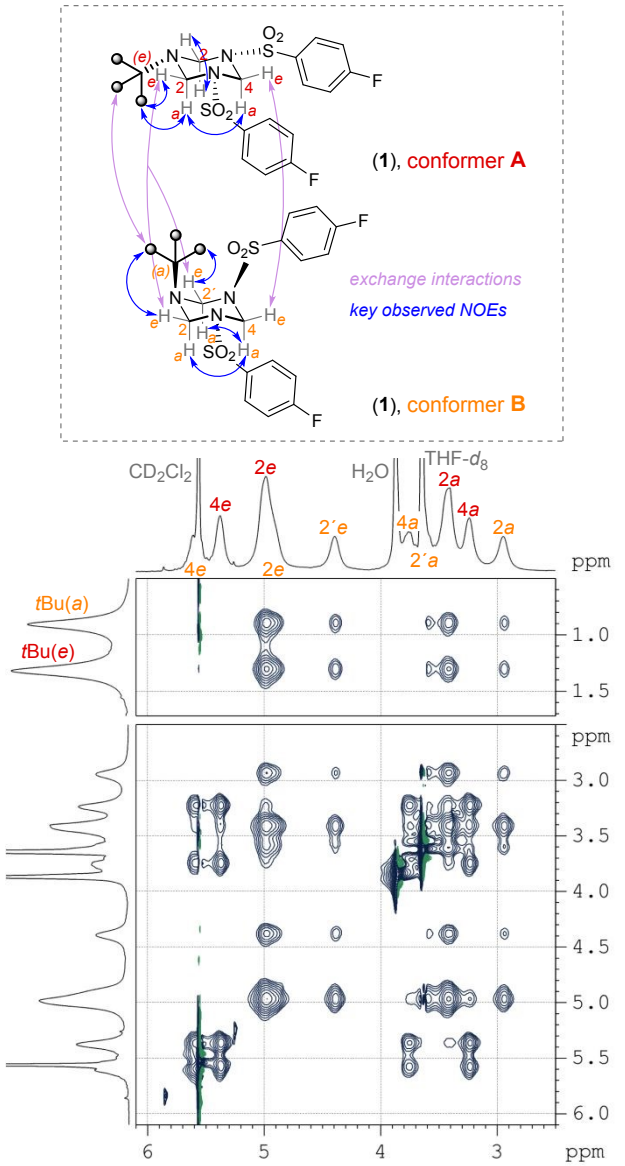

Fig. 7 Aliphatic region of the 2D ^{1}H EXSY / NOESY spectrum (mixing time = 100 msec) in THF-d_8/CD_2Cl_2 (v/v, 1:1) at –110 °C from triazinane **1**, proposed assignment of the signals (marked in color: red — conformer **A**, light orange — conformer **B**; conformer **C** is minor and not visible), and proposed analysis of the stereochemistry of main conformers **A** and **B** based on the NOE and exchange data (key interactions are indicated by color arrows at the top of the Figure). These interactions were extracted from a set of 2D NOESY / EXSY spectra with a range of mixing times from 50 to 600 msec using a protocol described in the text below.

The presence of conformer **C** was established as a result of the impossibility of performing deconvolution under the assumption that only two conformers **A**+**B** are mixed in the solution at any ratios of the Gaussian and Lorentzian waveforms.[16] As a result of the simulation during the deconvolution of conformers **A**+**B**, the presence of conformer **C** in the solution becomes apparent as a difference between the experimental spectrum and the sum of simulated **A**+**B** signals. It is also likely that conformer **C** is present in the THF-d_8/CD_2Cl_2 solution as well, but in smaller quantities, so it was difficult to unambiguously detect this structure (see also the ESI for details).

The exchange between conformers **A**–**C** and their configurations was studied using a set of EXSY / NOESY spectra with variable mixing times (from 50 to 600 msec) (Fig. 7). The very fast dynamic leads to an additional appearance of an array of intermolecular cross-peaks between different conformers, several consecutive NOE transfers, and to a negative sign of all cross-peaks. Nevertheless, after carefully studying the data the strong key NOE interactions between equatorial and axial *t*-Bu groups and corresponding protons of CH_2-fragments were revealed, which allowed to confirm the axial position of the *t*-Bu group in conformer **B** in solution. In addition, a number of other NOE and consecutive NOE interactions were observed, including a strong NOE between axial protons of different CH_2-groups (Fig. 7). The most significant NOE interaction is *t*-Bu···CH_2 with equatorial or axial protons for corresponding conformers (Fig. 7). It should be noted that the structure of conformer **C** is proposed and cannot be unambiguously established from NOESY spectra due to strong overlapping of signals and minor quantities in solution. However, despite that the axial orientation of the *t*-Bu group in it is hypothetic, the structure of conformer **C** is the most probable.

For such fast dynamic systems at low temperatures, a negative sign of NOE (the same as for exchange interactions and diagonal) is a common phenomenon. At any mixing time values, exchange interactions prevail in spectra with significant overlapping of signals. Therefore, its analysis is a laborious problem and quite far from commonly accepted processing. Moreover, a quantitative analysis of such NOESY spectra is impossible, only a qualitative assignment with quite low accuracy. A calculation of H···H distances is also impossible. After a full assignment of all signals in ^{1}H and 2D spectra by conventional processing, NOE can be distinguished from exchange interactions taking the following into consideration: exchange interactions are observed "intermolecularly" between the protons of two different conformers, while NOE interactions are observed "intramolecularly" between the protons in one conformer. The main NOE interaction is *t*-Bu···CH_2 (Fig. 7), which is impossible in the exchange variant. For a refinement, a parallel analysis of several NOESY spectra with different mixing times and a comparison of the cross-peaks intensities are required (see the ESI). The use of different mixing times leads to different contributions of NOE and exchange interactions in cross-peaks. However, there is always a chance of error during the analysis of such NOESY spectra, without any alternative variants.

The assignment sequence of the conformers and their stereochemistry was as follows: (1) a full assignment of all signals in ^{1}H/^{13}C/^{19}F spectra using 2D NMR techniques was performed; (2) integral intensities allowed to separate the signals of both conformers **A**/**B** existing in non-equimolar ratio; (3) ^{19}F NMR spectra allowed to uniquely identify conformer **B**, because it is the only one that has two different ^{19}F signals with equivalent intensities, in contrast with the other two conformers **A** and **C**; (4) using the isolated intense NOE interactions, the assignment of conformers **A**/**B** was refined and its stereochemistry was established (Fig. 7); (5) conformer C was minor and could only be identified by a residual principle, since NOE analysis provided only fragmentary information.

Triazinanes **2**–**4** show almost the same exact NMR dynamics with coalescence points ca. –95 °C (see the ESI) as for triazinane **1**, but with some different conformer ratios. However, they are much less soluble in the studied solvent systems than triazinane **1**, and they

DOI: 10.1039/D0OB01201C

don't have fluorine for ^{19}F NMR experiments. Due to the aforementioned fact, we have studied in detail triazinane **3** (*para*-Br substituted) (Fig. 8 and the ESI) as a representative example of a non-fluorinated derivative. Triazinane **3** has almost exactly the same ^{1}H NMR spectra at –110 °C (at which a separation of conformers is best) and the same signal assignments according to 2D ^{1}H–^{13}C edited-HSQC and ^{1}H–^{1}H EXSY/NOESY NMR data (see the ESI).

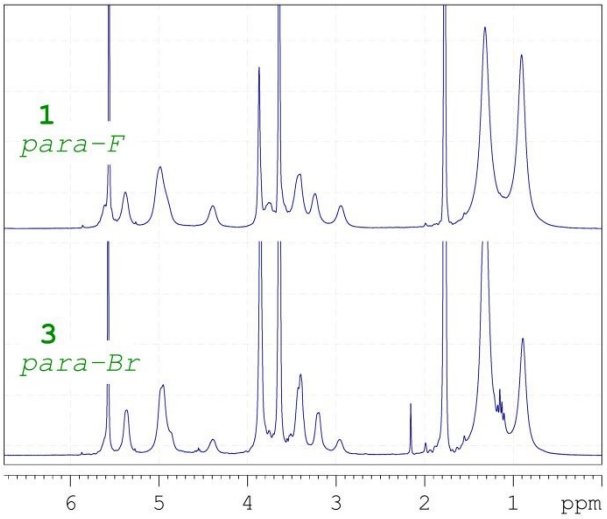

Fig. 8 Comparison of ^{1}H NMR spectra (aliphatic region) of the triazinane **1** (at the top) and triazinane **3** (at the bottom) in THF-d_8/CD_2Cl_2 (1:1) at –110 °C. It can be seen that they are quite similar except slightly different conformer ratio.

Hence, it was established during dynamic NMR experiments, that all-*e* conformer **A** is the most stable from the set of structures **A**–**F** and prevails in solutions of triazinanes **1**–**4** at temperatures below −100 °C, while only the conformer of type **C** with the axial *t*-Bu group is detected in the crystalline state (Scheme 5). It is important to note here that, unlike from the solution of 1,3,5-tris-*tert*-butyl-1,3,5-triazinane,[4] where the observation of *tert*-butyl in the axial position is associated with anomeric effect,[17] in this case we do not observe the related conformer as a strongly predominant one. This fact could probably be associated with the changed character of the nitrogen atoms attached to sulfonyl moieties.

Computational studies

To elucidate the facts mentioned above and to determine the energy barrier between the conformers carrying the *tert*-butyl group in the axial or equatorial positions, quantum chemical calculations were also performed. To achieve this goal, we have optimized at the B3LYP-D3/def2-TZVP level of theory (see ESI for details) both the axial and equatorial isomers of compound **1** (Hal = F) as a model for the whole series of the triazinanes **1–4**. Unexpectedly, the equatorial isomer is not a stationary point if the calculations are performed in the gas phase or using a continuum model of the THF solvent (see Fig. 9a), consequently the optimizations of both the equatorial and axial isomers lead to the same geometry, which is the axial isomer. In this regard, we were not able to estimate a very low energy barrier between the two conformers, wherein the discovered fact agrees well with the X-ray geometry of compound **1**. The reason for this behaviour is the formation of two intramolecular C–H···N bonds in the axial isomer that cannot be formed in the equatorial one (see Fig. 9a).

These H-bonds are further analysed below. The fact that the axial isomer is also the one that is obtained if the optimization is carried out in THF (continuum model) strongly disagrees with the experimental findings. However, the calculations using a continuum model are based in the dielectric constant, which is very small in THF and, therefore, there is not much difference with the calculations in the gas phase. To solve this issue, we included two explicit molecules of THF interacting with compound **1** and also utilized the continuum model (THF) during the optimization (see Fig. 9b). Interestingly, by using this more elaborated model, the equatorial isomer becomes stable and the axial isomer converges into the equatorial one. This result agrees well with the NMR experiments and gives an explanation for the different behaviour of this type of complexes in the solid state and solution. The THF molecules established several interactions with compound **1**. Some of them are indicated in Fig. 9b as dashed lines and it is worthy to highlight that the O-atom of one THF molecule interacts with the three axial H-atoms of the ring establishing three C–H···O contacts. The other THF also forms several C–H···O hydrogen bonding interactions both as donor and as acceptors.

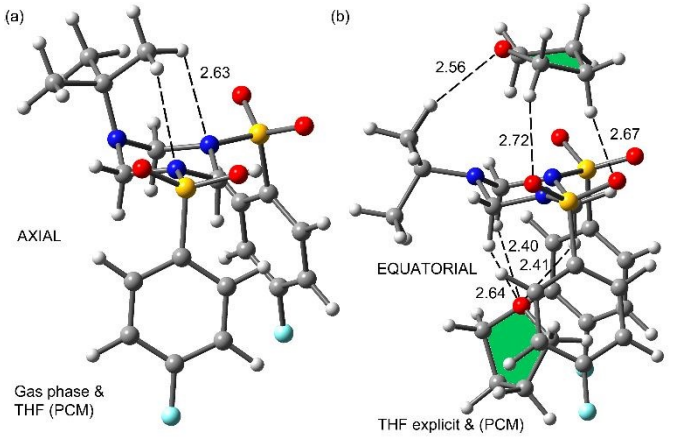

Fig. 9 B3LYP-D3/def2-TZVP optimized complex **1** in the gas phase and in THF (continuum model) (a); and also using two explicit THF molecules in the model (marked in green) (b).

We have performed the QTAIM (the quantum theory of atoms in molecules) analysis to evidence the existence of the intramolecular C–H···N hydrogen bonds in the axial isomer. The distribution of critical points (CP) and bond paths is given in Fig. 10 in two different perspectives. The existence of a bond path connecting two atoms is a universal indication of interaction.[18] The QTAIM analysis confirms the existence of both H-bonds that explains the stability of the axial isomer in this type of compounds. Each H-bond is characterized by one bond CP (green sphere) and bond path interconnecting the H and N-atoms. Moreover, we have estimated the energy of each H-bond by using the V(r) predictor.[19] The dissociation energy of each H-bond is 2.8 kcal/mol, thus supporting the formation of

the axial isomer, since the energy of both H-bonds compensate the axial-equatorial energy difference (in this system it is not possible to compute because the equatorial is not a minimum and converges to the axial isomer).

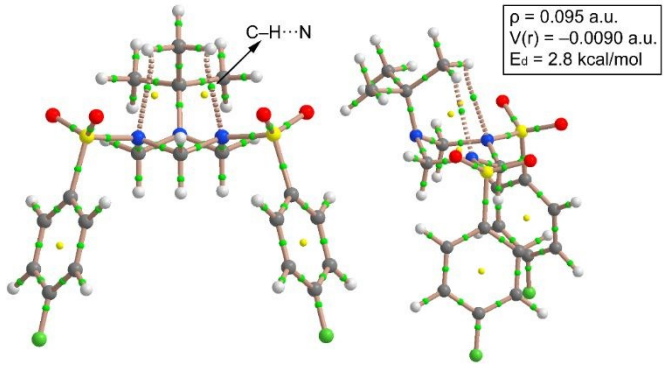

Fig. 10 QTAIM analysis of the axial isomer of the fluorine-substituted triazinane **1**. The dissociation energy using the V(r) predictor and the ρ and V(r) parameters are indicated on the right.

Hereby, in the final part of this work, we have ascertained the presence and the significant role of intramolecular C–H···N hydrogen bonds, which, probably, along with the anomeric effect of lone electron pairs of the nitrogen atoms, known for such systems,[17] stabilize the conformers with the axial orientation of the *tert*-butyl group.

Concluding Remarks

Six X-ray analyses of triazinane derivatives **1**–**4** revealed a previously undescribed case of the axial position of the *tert*-butyl group in the chair conformation of the unconstrained 1,3,5-triazinane ring in the solid phase and confirmed the theoretical predictions formulated earlier. This discovery enlarges a very small family of unanchored *tert*-butyl group-bearers in the solid phase and also highlights an important conformational characteristic of 1,3,5-triazinane framework useful for consideration during crystals design.[20] On the contrary, it was detected that the conformers with an equatorial arrangement of all substituents predominate in solutions at temperatures below −100 °C. The role of intramolecular hydrogen bonding in the stabilization of the *tert*-butyl group axial position in a 1,3,5-triazinane ring is highlighted.

It is noteworthy that this investigation along with those cases briefly summarized above where a *tert*-butyl group occupies an axial position of six-membered saturated heterocycles, indicate that traditionally used steric scale of substituents, developed on the basis of monosubstituted cyclohexanes, e.g. “A-value”, is hardly applicable for such systems.[21] In this regard, a challenge towards the creation of an alternative steric scale for the substituents in “non-innocent” heterocyclic systems rises.

Acknowledgements

View Article Online
DOI: 10.1039/D0OB01201G

The publication has been prepared with the support of the "RUDN University Program 5-100" and Russian Foundation for Basic Research (project No 19-03-00807a). The XRD measurements were performed using equipment of CKP FMI IPCE RAS. AF thanks the MICIU/AEI (project CTQ2017-85821-R FEDER funds) for financial support. We thank Llorenç Rigo (CTI, UIB) for technical assistance.

Conflicts of interest

There are no conflicts to declare.

Notes and references

1 (a) I. Kolossvary and W. C. Guida, *J. Am. Chem. Soc.,* 1993, **115**, 2107; (b) D. H. R. Barton and R. C. Cookson, *Q. Rev. Chem. Soc*., 1956, **10**, 44; (c) K. B. Wiberg, J. D. Hammer, H. Castejon, W. F. Bailey, E. L. DeLeon and R. M. Jarret, *J. Org. Chem*., 1999, **64**, 2085; (d) E. Juaristi, in Conformational Behavior of Six-Membered Rings; VCH Publishers: New York, 1995; (e) E. L. Eliel, and S. H. Wilen, in Stereochemistry of Organic Compounds; Wiley: New York, 1994; pp 665–834 and references therein.

2 E. L. Eliel Sr. and M. C. Knoeber, *J. Am. Chem. Soc.,* 1966, **88**, 5347.

3 L. Angiolini, R. P. Duke, R. A. Y. Jones and A. R. Katritzky, *J. Chem. Soc. B*, 1971, 1308.

4 J. G. Jewett, J. J. Breeyear, J. H. Brown and C. H. Bushweller, *J. Am. Chem. Soc.,* 2000, **122**, 308.

5 (a) F. W. Vierhapper; E. L. Eliel and G. Zuniga, *J. Org. Chem.,* 1980, **45**, 4844; (b) J. M. Lehn, F. G. Riddell, B. J. Price and I. O. Sutherland, *J. Chem. Soc., B*, 1967, 387; (c) L. Angiolini, R. P. Duke, Richard A. Y. Jones and A. R. Katritzky, *J. Chem. Soc., Perkin Trans. 2*, 1972, 674; (d) K. Pihlaja, *J. Chem. Soc., Perkin Trans. 2*, 1974, 890; (e) K. Bergesen, B. M. Carden and M. J. Cook *J. Chem. Soc., Perkin Trans. 2*, 1976, 345; (f) V. J. Baker, I. J. Ferguson, A. R. Katritzky, R. Patel and S. Rahimi-Rastgoo, *J. Chem. Soc., Perkin Trans. 2*, 1978, 377; (g) F. W. Vierhapper and E. L. Eliel, *J. Org. Chem.,* 1979, **44**, 1081; (h) W. G. Bentrude and J. H. Hargis, *J. Am. Chem. Soc.,* 1970, **92**, 7136.

6 (a) S. Antúnez and E. Juaristi, *J. Org. Chem.,* 1996, **61**, 6465; (b) G. Gill, D. M. Pawar and E. A. Noe, *J. Org. Chem*., 2005, **70**, 10726; (c) J.-H. Lii, K.-H. Chen, K. A. Durkin and N. L. Allinger, *J. Comput. Chem.,* 2003, **24**, 1473.

7 (a) H. Lamraoui, A. Messai, D. Bilge, M. Bilge, A. Bouchemma and C. Parlak, *J. Mol. Struct*., 2017, **1138**, 64; (b) C. Sicking, A. Mix, B. Neumann, H.-G. Stammler and N. W. Mitzel, *Dalton Trans*., 2012, **41**, 104; (c) A. Rivera, O. L. Torres, J. D. Leiton, M. S. Morales-Rios and P. Joseph-Nathan, *Synth. Commun*., 2002, **32**, 1407.

8 R. Gilardi, R. N. Evans and R. Duddu, *Acta Cryst*., 2003, **E59**, o1187.

9 (a) R. W. Warrent, C. N. Caughlan, J. H. Hargis, K. C. Yee and W. G. Bentrude, *J. Org. Chem.,* 1978, **43**, 4266; (b) P. Geneste, J.-M. Kamenka, R. Roques, J. P. Declercq and G. Germain, *Tetrahedron Lett.,* 1981, **22**, 949; (c) L. J. McCormick, C. McDonnell-Worth, J. A. Platts, A. J. Edwards and D. R. Turner, *Chem. Asian J.,* 2013, **8**, 2642; (d) K. D. Hargrave and E. L. Eliel, *Tetrahedron Lett.,* 1979, **20**, 1987; (e) A. Majumdar and R. H. Holm, *Inorg. Chem*., 2011, **50**, 11242.

10 K. Sparrow, D. Barker and M. A. Brimble, *Tetrahedron*, 2012, **68**, 1017.

View Article Online
DOI: 10.1039/D0OB01201G

11 (a) B. A. Shainyan, I. A. Ushakov, A. Koch and E. Kleinpeter, *J. Org. Chem*., 2006, **71**, 7638; (b) E. Ziegler and W. Ruef, *Z. Naturforsch. B Chem. Sci*., 1975, **30**, 951; (c) J. L. Lee, K. C. Ahn, O. S. Park, Y. K. Ko and D.-W. Kim, *J. Agric. Food Chem.,* 2002, **50**, 1791; (d) O. O. Orazi, R. A. Corral and R. Bravo, *J. Heterocyclic Chem*., 1986, **23**, 1701; (e) A. V. Kletskov, D. M. Gil, A. Frontera, V. P. Zaytsev, N. L. Merkulova, K. R. Beltsova, A. A. Sinelshchikova, M. S. Grigoriev, M. V. Grudova and F. I. Zubkov, *Crystals*, 2020, **10**, 369; (f) D. Liang, W.-J. Xiao and J.-R. Chen, *Synthesis*, 2020, **52**, in press (DOI: 10.1055/s-0040-1707160).
12 (a) R. F. W. Bader, *Chem Rev*, 1991, **91**, 893; (b) C. M. Breneman and L. W. Weber, *Can. J. Chem*., 1996, **74**, 1271; (c) B. A. Caine, M. Bronzato and P. L. A. Popelier, *Chem. Sci*., 2019, **10**, 6368.
13 D. Casarini, L. Lunazzi, A. Mazzanti, *Eur. J. Org. Chem.*, 2010, 2035–2056.
14 J. S. Siegel, *J. Org. Chem.*, 1988, **53**, 2629–2630.
15 T. Olsson, D. Tanner, B. Thulin, O. Wennerstrom, *Tetrahedron*, 1981, **37**, 3473–3483.
16 (a) R. A. Novikov, D. A. Denisov, K. V. Potapov, Y. V. Tkachev, E. V. Shulishov and Y. V. Tomilov, *J. Am. Chem. Soc*., 2018, **140**, 14381; (b) R. A. Novikov, K. V. Potapov, D. N. Chistikov, A. V. Tarasova, M. S. Grigoriev, V. P. Timofeev, Y. V. Tomilov, *Organometallics*, 2015, **34**, 4238.
17 I. V. Alabugin, in Stereoelectronic Effects. A Bridge between Structure and Reactivity, Wiley, 2016, p. 137.
18 R. F. W. Bader, J. *Phys. Chem. A*, 1998, **102**, 7314.
19 E. Espinosa, E. Molins and C. Lecomte, *Chem. Phys. Lett*., 1998, **285**, 170.
20 M. I. P. Reis, G. A. Romeiro, R. N. Damasceno, F. C. da Silva and V. F. Ferreira, *Rev. Virtual Química*, 2013, **5**, 283.
21 M. Mancinelli; G. Bencivenni; D. Pecorari; A. Mazzanti, *Eur. J. Org. Chem,* 2020, **2020**, 4070.